CREEP CRACK GROWTH ANALYSIS BASED ON MICROSCOPIC FRACTURE MECHANISM

M. Tabuchi[1], K. Kubo[1], K.Yagi[1] and A. T. Yokobori, Jr.[2]

[1]National Institute for Materials Science, Sengen, Tsukuba, 305-0047, Japan
[2]Tohoku University, Aoba, Sendai, 980-8579, Japan

ABSTRACT

Relationship between creep crack growth rate and microscopic fracture mechanism i.e., wedge-type intergranular, transgranular and cavity-type intergranular crack growth, has been investigated on Alloy 800H and 316 stainless steel. The growth rate of wedge-type and transgranular creep crack could be characterized by creep ductility. Creep damages formed ahead of the cavity-type creep crack tip accelerated the crack growth rate. Based on the experimental results, FEM code that simulates creep crack growth taking the fracture mechanism into account has been developed. The effect of creep ductility and void formation ahead of the crack tip on creep crack growth rate could be evaluated.

KEYWORDS

Creep crack growth, Alloy 800H, 316 stainless steel, Creep fracture mechanism, C^* parameter, FEM analysis, Vacancy diffusion

INTRODUCTION

Understanding of creep crack growth behavior is important for the reliability evaluation of high temperature structural components. Creep crack growth properties are affected by microscopic fracture mechanism dependent on temperature and loading condition. For the long-term services, evaluation of creep crack growth by grain boundary cavitation [1] is important. Type IV creep crack in heat affected zone of welded components grows accompanied by void formation ahead of the crack tip [2]. It would be necessary to evaluate the creep crack growth behavior, taking microscopic features such as damage formation into account, for the accurate life prediction.

In the present work, creep crack growth tests were conducted using CT specimen of Alloy 800H and 316 stainless steel at various temperature and loading conditions. Creep crack growth behavior was characterized in terms of microscopic creep fracture mechanism. In order to evaluate the relations between creep crack growth rate and fracture mechanism, FEM analysis taking the creep ductility and void formation into account was conducted.

EXPERIMENTAL PROCEDURES

Materials tested are Alloy 800H and 316 stainless steel plates. Chemical composition of Alloy 800H is given in Table 1. The solid solution heat treatment condition was 0.4h at 1443K. Creep crack growth tests were conducted using CT specimen of 50.8mm in width and 12.7mm in thickness. Fatigue pre-crack of 2.5mm was introduced at room temperature. After fatigue pre-cracking, side-grooves of 20% of thickness were machined. Creep crack length was measured using D.C. electrical potential technique. Load line displacement between upper and lower clevises, which connect the specimen with pull rods, was measured. The creep crack growth tests were conducted at temperature range from 873K to 1073K.

TABLE 1
CHEMICAL COMPOSITION OF ALLOY800H (MASS%)

C	Si	Mn	Fe	S	Ni	Cr	Cu	Ti	Al
0.06	0.4	1.0	45.4	0.001	31.9	20.0	0.03	0.46	0.35

RESULTS AND DISCUSSION

Creep Fracture Mechanisms

Figure 1 shows microscopic features of creep cracks observed in CT specimens of Alloy 800H. Three types of creep crack growth, wedge-type intergranular, cavity type intergranular and transgranular crack growth were observed depending on testing temperature and loading conditions. For higher stresses at lower temperatures, intergranular fracture due to the wedge-type cracking (W-type) was observed. It is considered that fine γ' precipitates hardened the matrix and brittle wedge-type fracture was occurred at this testing condition. For lower stresses at higher temperatures, intergranular fracture due to the formation of cavities at the interface between matrix and $M_{23}C_6$ precipitates on grain boundaries (C-type) was observed. Large creep damaged zone ahead of the crack tip was observed for C-type crack growth. Transgranular fracture (T-type) was observed between the temperature and loading conditions of W-type and C-type.

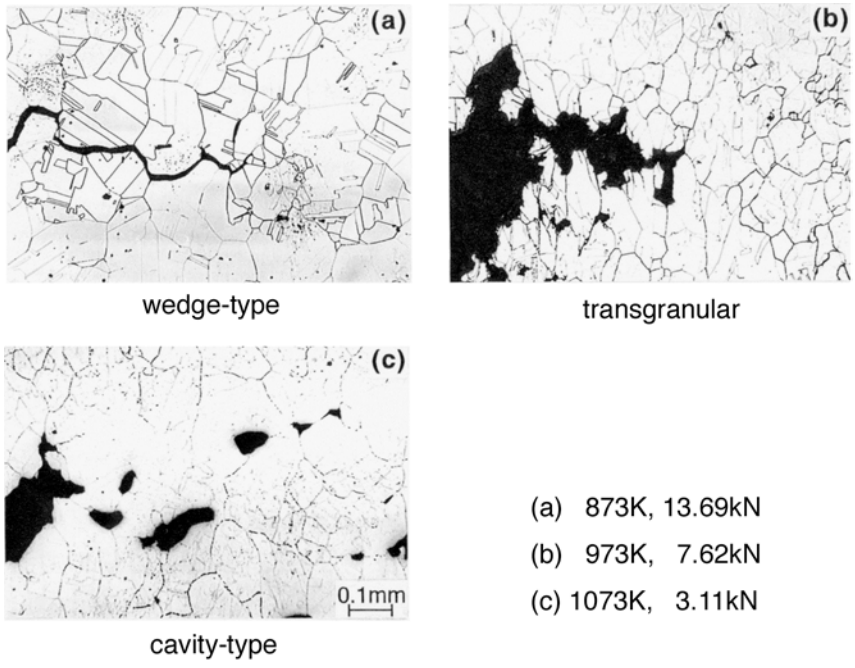

Figure 1: Microscopic features of creep cracks observed in CT specimens creep interrupted of Alloy 800H.

Relationship between Creep Crack Growth Rate and Fracture Mode

Creep crack growth rate was evaluated by C^* parameter calculated as follows [3];

$$C^* = \frac{n}{n+1} \frac{P\dot{\delta}}{B_N (W-a)} \left(\gamma - \frac{\beta}{n} \right) \qquad (1)$$

where, W is the specimen width, a is the crack length, P is the load, B_N is the net thickness, $\dot{\delta}$ is the load line displacement rate, n is the creep exponent in Norton's rule and γ and β are the function of a and W. The value of n was obtained from the relations between minimum creep rate *vs*. applied stress for round bar creep specimens.

The relationship between creep crack growth rate, *da/dt*, and C^* parameter obtained under relevant creep fracture mechanism condition for Alloy 800H is shown in Figure 2. The crack growth data of initial tail parts [4] were omitted in this figure. The *da/dt vs*. C^* relations depend on the microscopic creep crack growth mechanism. The creep crack growth rate for W-type and C-type fracture mode was higher than that for T-type fracture mode. The creep crack growth rate for C-type mode exists between the upper bound for W-type and the lower bound for T-type mode.

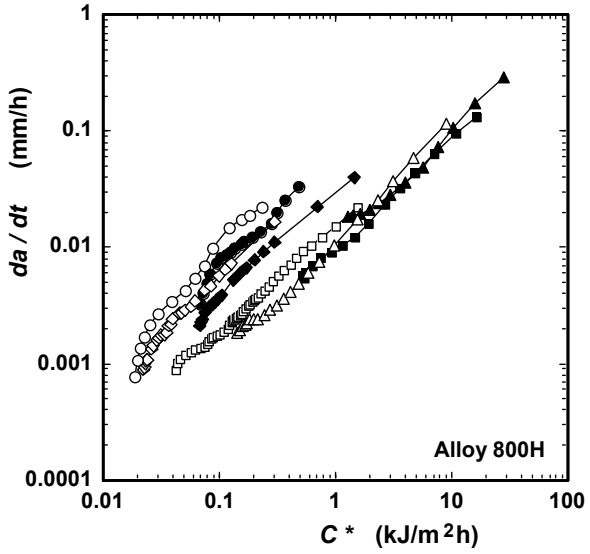

	Temp. (K)	Load (kN)	Fracture mode
●	873	13.69	W
○		11.47	W
▲	923	11.71	T
△		8.98	T
■	973	7.62	T
□		4.36	T
◆	1073	3.11	C
◇		2.61	C

Figure 2: Relationship between creep crack growth rate, *da/dt*, *vs*. C^* parameter.

Creep ductility was dependent on creep fracture mechanism, and that was lower for W-type, higher for T-type, and medium for C-type fracture mode. It is considered that difference of creep ductility between fracture modes is one of the reasons why *da/dt* depends on creep fracture mode. Figure 3 shows the relationship between creep crack growth rate at C^*=1 kJ/m^{2}h *vs*. reduction of area for round bar creep specimens of Alloy 800H and 316 stainless steel. These relations were dependent on creep fracture mechanisms. For W-type and T-type fracture mode, the *da/dt* was inversely proportional to creep ductility as shown with the solid curve in Figure 3. Creep crack growth rate for W-type and T-type mode could be written as follows [5];

$$\frac{da}{dt} = \frac{6.26 \times 10^{-3}}{\varepsilon_f^*} C^{*0.92} \qquad (2)$$

where, ε_f^* is the creep ductility.

For C-type fracture mode, however, *da/dt* was faster than that predicted from the equation (2). The *da/dt* was accelerated as the testing temperature and time was increased for C-type fracture mode. When creep voids are not formed ahead of the crack tip such as W-type and T-type fracture mode, the creep crack growth rate could be characterized by the creep ductility. When many voids and micro cracks are formed ahead of the main crack tip, the creep crack growth rate was accelerated than that predicted from creep ductility. In order to predict the creep crack growth rate under C-type fracture mode, it is necessary to consider not only creep ductility but also the effect of creep damages ahead of the crack tip. Vacancy diffusion and void formation accelerated under multi-axial condition at higher temperature should be taken into account.

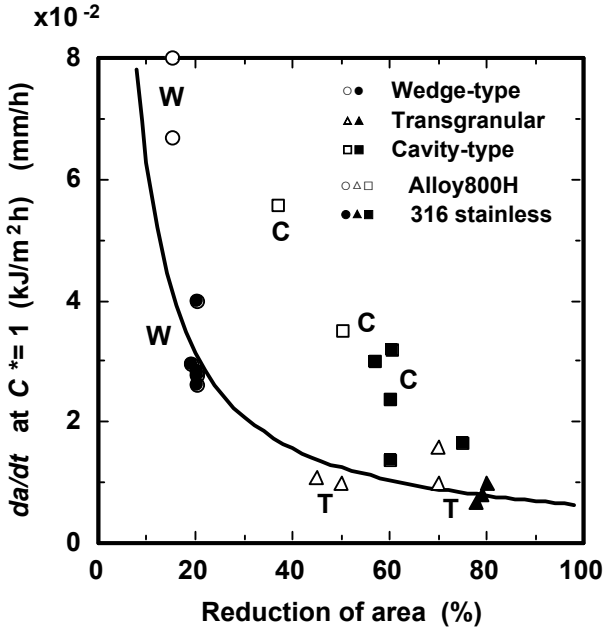

Figure 3: Relationship between *da/dt* at C^*=1 kJ/m^{2}h vs. creep ductility.

Computational Simulation for Creep Crack Growth

We attempted to simulate creep crack growth behavior taking the fracture mechanism into account on the basis of experimental results. The FEM analytical model of CT specimen is shown in Figure 4. For W-type and T-type fracture mode, the *da/dt* was inversely proportional to creep ductility, therefore the crack growth could be characterized by critical strain condition. The creep strain distribution of CT specimen model was calculated by FEM. When the equivalent creep strain ahead of the crack tip reached to the critical value, which is the creep ductility of round bar specimen, the coordinate of the crack tip node was moved according to he method proposed by Hsu et al. [6]. The C^* line integral was calculated for every time step.

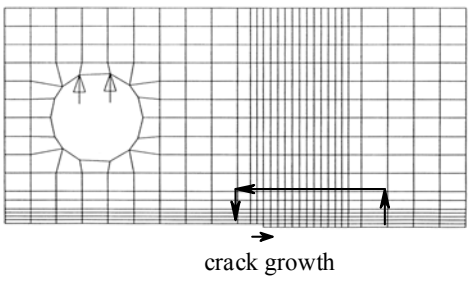

Figure 4: Analytical model for creep crack growth.

An example of computational and experimental relation of creep crack growth rate *vs.* C^*

integral is shown in Figure 5. The symbols indicate experimental data and the bold line shows the calculated results. In this case of T-type fracture mode, the crack growth rate could be predicted from Norton's creep rule and creep fracture strain. If we use half value of fracture strain for fracture criteria, the twice value of *da/dt* was obtained as shown with dashed line in Figure 5. These computational results coincide with the experimental ones that *da/dt* is inversely proportional to creep ductility.

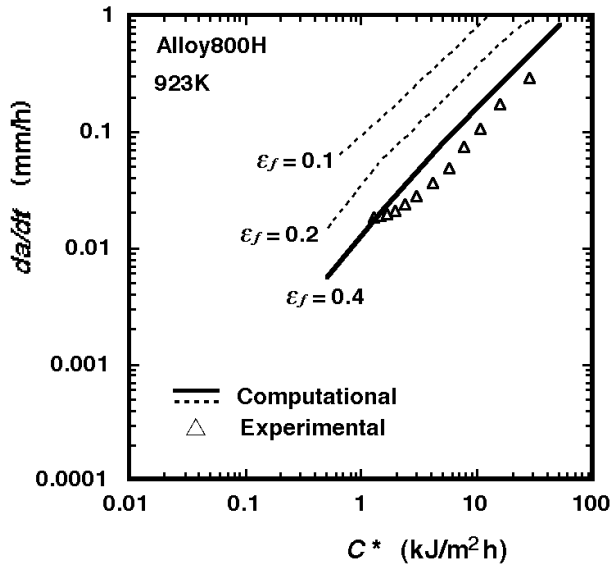

Figure 5: Comparison of experimental and computational relation between *da/dt vs. C** parameter.

For C-type fracture mode, which was observed at higher temperatures, *da/dt* was faster than others due to the formation of voids ahead of the crack tip. In order to evaluate the effect of void formation for C-type mode, it would be necessary to analyze the crack growth taking vacancy diffusion into account under multi-axial condition. The vacancy diffusion equation under stress gradient is given as follows [7, 8];

$$\frac{\partial C}{\partial t} = D\nabla\left(\nabla C + \frac{C\nabla V}{RT}\right) \qquad (3)$$

$$V = -\sigma_p \, \Delta v \qquad (4)$$

where, C is the vacancy concentration, D is the diffusion coefficient, σ_p is the hydrostatic stress and Δv is the volume changes by vacancy diffusion. In the present computational simulation, the vacancy

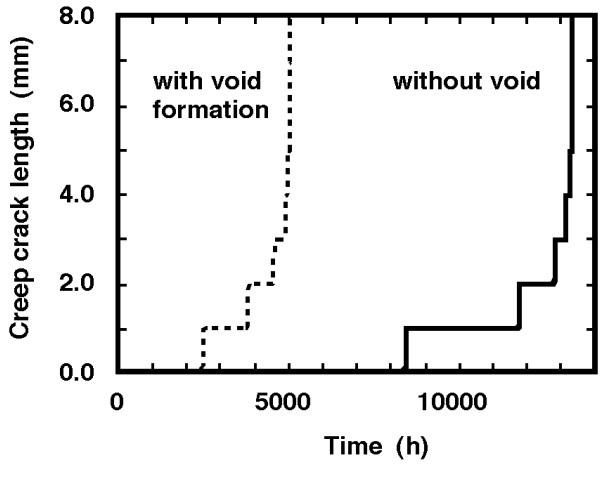

Figure 6: Example for simulation of creep crack growth
taking the diffusion into account.

concentration ahead of the crack tip is calculated by FEM according to the equations (3) and (4), and if that value reaches to the critical value, the stiffness matrix [K] is decreased step by step. The creep crack growth is simulated by combining the critical strain criteria and vacancy diffusion criteria. Figure 6 shows an example calculated by assuming that D=12.7e^{-11}(m^2/s), Δv=2.0e^{-6}(m^2/mol) and critical vacancy concentration C/C_0 =1.25. The qualitative results that creep crack initiation time and crack growth rate were accelerated were obtained while taking the void formation ahead of the crack tip into account. The quantitative evaluation for the effect of vacancy diffusion on crack initiation and growth under multi-axial condition should be the future work.

CONCLUSIONS

Creep crack growth tests have been carried out using CT specimens on Alloy 800H and 316 stainless steel at various testing conditions. The relationship between creep fracture mechanism and creep crack growth behavior has been investigated. The results are summarized as follows;
(1) Three types of creep crack growth mechanisms, i.e., wedge-type intergranular, transgranular and cavity-type intergranular, were observed for Alloy 800H and 316 stainless steel depending on testing conditions.
(2) Creep crack growth rate was dependent on microscopic creep fracture mechanism. The growth rate of wedge-type and cavity-type intergranular creep crack was higher than that of transgranular creep crack.
(3) The growth rate of wedge-type and transgranular creep crack could be characterized by creep ductility. The creep damages formed ahead of the cavity-type creep crack were considered to accelerate the crack growth rate.
(4) The FEM code, which simulates creep crack growth taking the fracture mechanism into account, has been developed. The effect of creep ductility and void formation ahead of the crack tip due to the vacancy diffusion on creep crack growth rate could be evaluated.

References

1. Riedel, H. (1986) *Fracture at High Temperatures,* Springer-Verlag, Berlin.
2. Tabuchi, M., Watanabe, T., Kubo, K., Matsui, M., Kinugawa, J. and Abe, F. (2000) *Proc. of 2nd HIDA Conference*, Stuttgart, Germany, S2-4.
3. Ernst, H.A. (1983) *ASTM STP* 791, I-499.
4. Yokobori, A.T. and Yokobori, T. (1988) *Eng. Frac. Mech.* 31, 931.
5. Nikbin, K.M., Smith, D.J. and Webster, G.A. (1986) *Trans. ASME, J. Eng. Mater. Tech.* 108, 189.
6. Hsu, T.R. and Zhai, Z.H. (1984) *Eng. Fract. Mech.* 20, 521.
7. Yokobori, A.T., Jr, Nemoto, T., Sato, K. and Yamada, T. (1993) *Japan Soc. Mech. Eng.* 59, 104.
8. Kikuchi, K. and Kaji, Y. (1995) *Proc. of 33rd Symposium on Strength of Materials at High Temperatures*, Yokohama, Japan, 1.